euspen's 24th International Conference & Exhibition, Dublin, IE, June 2024
www.euspen.eu

Attenuation of thermographic disturbances emitted from a high-sensitivity sensor

HyungTae Kim[1], Kwon-Yong Shin[1], Jun Yong Hwang[1] & Heuiseok Kang[1]

[1]*Research Institute of Human-Centric Manufacturing Technology, KITECH, Sangrok, Ansan, Gyeonggi, South Korea*

htkim@kitech.re.kr

Abstract
A thermographic image usually provides a large field-of-view (FOV) with high temperature sensitivity; thus it has great potential for the inspection of panel devices such as flat panel displays (FPDs), wafers, and photovoltaic elements. However, the high reflectivity and high sensitivity of panel devices can lead to the shape of the thermal camera itself being detected in the thermographic image. Thus, long-wave infrared rays (LWIR) from the thermal camera should be removed for accurate thermography of reflective devices. This study investigated the attenuation of the LWIR from the front of the reflective surfaces. The proposed structure was similar to the coaxial optics in a microscope, and polished LWIR filters were tested as half mirrors within the coaxial optics. Thermal uniformity in the dark state was considered for the removal of LWIR within the thermal camera, and thermographic images of an ink stain were investigated when an LWIR source was applied.

Image, optical, visual inspection, temperature

1. Introduction

Thermography visualises long-wave infrared rays (LWIR), which exhibits quite different characteristics from visible rays (VIS), being able to penetrate media opaque to visible light. Thus, thermography reveals invisible or hidden phenomena as visible patterns, and has become popular in industrial applications such as the detection of gas leakages and mechanical failure [1].

Thermography is primarily intended to capture the thermal emission of arbitrary objects in the field of view (FOV); however, false images are frequently captured owing to thermal reflection. The LWIR creating these images originates from the surroundings rather than from within the FOV, and is reflected on the surfaces of objects in the FOV. Thermal reflection usually occurs on polished surfaces and is generally stronger than VIS reflection [2]. To address the resultant false images, which cause confusion at industrial sites, the removal of thermal reflection has been discussed in some studies. The simplest method for removing LWIR is background subtraction from time-varying thermal images [3]; background subtraction can be used for surveillance, but is ineffective for stationary objects. Deep learning and artificial intelligence (AI) have also been applied to remove thermal reflections [4]; however, AI requires sample images for training and the removal results are not guaranteed. Thermal camera companies have recognised the problem of reflection: they recommend changing the camera positions and angles when capturing images of reflective objects to prevent direction frontal reflection [5]; furthermore, a frontal image can be synthesised using multiple images from different incidence angles. Polarisation is the most popular method for reflection removal [6]; however, it requires an oblique incidence angle. Thus, the polarisation method is disadvantageous for frontal image acquisition.

Thus, the attenuation of frontal thermal reflection using conventional optical filters was investigated in this study. Briefly, a thermographic image of an ink stain in front of a polished silicon wafer was acquired, and LWIR-pass filters and an LWIR source were placed between the wafer and the camera ,similar to a half-mirror. The proposed structure is typical of coaxial optics used to bypass the LWIR from a camera.

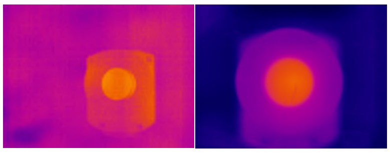

Figure 1. Thermographic images focused on polished surfaces of a silicon wafer (left) and an LWIR-pass filter (right) reflecting a camera.

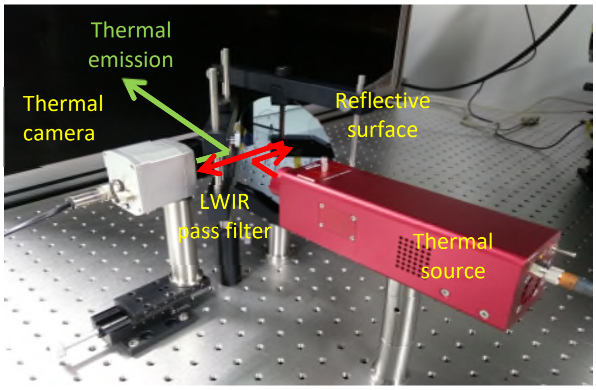

Figure 2. Experimental apparatus to remove thermal reflection.

2. Materials and method

As the thermal sensitivity of a thermal camera increases, thermal reflection becomes important in the inspection of precisely processed products. Figure 1 shows the thermal images from a camera directed at a silicon wafer and a LWIR-pass filter, showing that the thermal emission from the camera is visible due to reflection. The silicon wafer is opaque to LWIR; however, the LWIR-pass filter is transparent according to its specifications. Both surfaces were polished, and thermal reflections were observed in both images, despite the LWIR transparency of the filter. In the case of the LWIR-pass filter, the shapes behind the filter were also captured; thus, the filter can be used as a half-mirror. Figure 2 shows that the structure of the coaxial optics eliminates unwanted thermal reflection. The emissions from the thermal camera are deflected out of the system by the half-mirror. The thermal radiation from the LWIR source is also deflected by the filter, and reflected from the target surface. Subsequently, the reflected LWIR passes through the filter and arrives at the thermal camera. Thus, the image of the thermal camera is removed from the thermographic image.

In a coaxial structure, the transmissibility and reflectivity of the filter with respect to the LWIR are crucial. The LWIR transmissibility can be obtained from the spectral responses of the material and LWIR reflection is achieved by polishing the surface. After investigating the transmissibility, Potassium Bromide (KBr), Germanium (Ge), Barium Fluoride (BaF_2) and Sodium Chloride (NaCl) were chosen as half mirrors. The reflection removal performance can be measured by observing the uniformity of a thermographic image in IR darkness. When inspecting a blank wafer, the uniformity of the image increases when false images are removed, because the deviation among the image pixels decreases. The uniformity can be conventionally calculated using the average (μ) and standard deviation (σ) of the image pixels as follows.

$$\gamma = 1 - \sigma/\mu \quad (1)$$

3. Experiments

The experimental apparatus was constructed with a thermal camera (Optris PI640, Δ=40mK), an LWIR source (Thorlabs SLS203L), an LWIR-pass filter, an industrial controller (Beckhoff CX2020) and a silicon wafer on an optical table. The surfaces of the filter and wafer were polished. Printed patterns and an ink stain were drawn on the wafer. The camera was placed in front of the wafer and the LWIR source was vertically installed on the right side. The filter was set close to the thermal camera to cover the lens. The filter was attached to a rotatable post to enable adjustment of the incidence angle of the LWIR source and the thermal camera. The filter was transparent under VIS conditions and covered the thermal lens in front of the camera. The materials of the filters in the experiment were selected to have the LWIR transmission range between 8 and 14µm, such as KBr, Ge, BF_2 and NaCl. The LWIR from the source was reflected on the back side of the filter, and arrived at the wafer. The reflected LWIR on the wafer passed through the filter and was captured using the thermal camera. Thermographic images were acquired after rotating the filter by 0° and 45°. The source was then activated to investigate the ink stain on the wafer. The thermographic images were stored in an industrial controller and image processing was performed using OpenCV.

4. Results and discussion

Reflection removal was observed when using KBr, Ge, BaF_2 and NaCl filters. The float glass filter exhibited no response because of the spectral range of transmission. Figure 3 shows the thermographic images obtained using the Ge filter. When the angle of the Ge filter was 0°, the brightness range owing to reflection became larger than that without the filter. The brightness range decreased when the Ge filter was rotated by 45°. After applying the LWIR source, the line written using ink became conspicuous. This indicates that the LWIR from the camera was bypassed and the ink stain on the wafer became clear. The other filters also exhibited this effect during the experiments. Table 1 lists the variations in uniformity according to the rotation angle and material of the LWIR filters. At 0°, the uniformities with the filters were greater than those without the filters. Because the filters were placed near the camera, the thermal reflection of each filter was stronger than that of the wafer. After rotating the filters by 45°, the uniformity increased, indicating that the false images were reduced. Therefore, the proposed method is effective in removing thermal reflections when the thermal camera is placed in front of the inspection area. Moreover, thermal inspection of the semiconductor and flat panel displays from the front was possible using the proposed method. Finally, the best results in the removal of thermal reflection were attained using the Ge filter; however, the removal performance could possibly be increased using another material. In the future, we plan to develop new materials for LWIR half-mirrors.

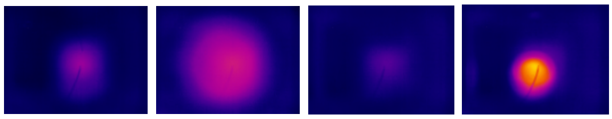

(a) (b) (c) (d)

Figure 3. Thermographic images of reflective surface (a) without filter (b) with 0° Ge filter (c) with 45° Ge filter; and (d) with 45° Ge filter and an LWIR source.

Table 1 Uniformity according to rotation and LWIR filters

Angle	Free	KBr	Ge	BaF_2	NaCl
0°	0.5561	0.4500	0.5053	0.5287	0.5497
45°	-	0.5812	0.7475	0.6293	0.5871

5. Conclusion

This study presents a method for removing the false image of a thermal camera in front of an inspection target. A false image is created by thermal reflection when a thermal camera is placed in front of a reflective surface. Because this phenomenon disturbs temperature measurement, the false image is customarily removed using conventional coaxial optics. In this study, LWIR filters were applied to the half mirror in a coaxial optics system. The consequent image-removal performance was verified in terms of the uniformity of the thermographic images. The LWIR filters generally reduced the false image from the thermal reflection. The Ge filter exhibited the best removal performance among all filters used in the experiment. The proposed method can be applied to the front thermal inspection of reflective products.

Acknowledgement

This study has been conducted with the support of the Korea Institute of Industrial Technology as “Development of root technology for multi-product flexible production (PEO24090)”.

References

[1] Resendiz-Ochoa E, Osornio-Rios R A, Benitez-Rangel J P, Romero-Troncoso R J and Morales-Hernandez L A 2018 Induction Motor Failure Analysis: An Automatic Methodology Based on Infrared Imaging *IEEE Access* **6** 76993-77003

[2] Liu R and Vondrick C 2023 Humans as Light Bulbs: 3D Human Reconstruction from Thermal Reflection *Proc. IEEE/CVF CVPR* 12531-12542

[3] Zeise B and Wagner B 2016 Temperature Correction and Reflection Removal in Thermal Images using 3D Temperature Mapping *Proc ICINCO* **2** 158-165

[4] Batchuluun G, Baek N R, Nguyen D T, Pham T D, and Park K R 2020 Region-based removal of thermal reflection using pruned fully convolutional network *IEEE Access* **8** 75741–75760

[8] Beall E and Prairie E 2018 Systems and approaches for thermal image corrections *United States Patent* 10,129,490 B2

[9] Li N, Zhao Y, Pan Q AND Kong S G 2018 Removal of reflections in LWIR image with polarization characteristics *Optics Express* **26** 16488